

Chapter 4

The Lipid Cubic Phase as a Medium for the Growth of Membrane Protein Microcrystals



Zina Al-Sahouri, Ming-Yue Lee, Dianfan Li, Wei Liu, and Martin Caffrey

4.1 Introduction

SFX¹ Serial femtosecond X-ray crystallography (SFX) is a relatively new method for collecting crystallographic information on small crystals fed continuously across a free-electron laser (FEL) beam composed of high-fluence X-ray bunches femtoseconds long [2, 3]. Each encounter between an X-ray bunch and a microcrystal (*hit*) ideally gives rise to a single, still diffraction pattern with greater than 15 measurable reflections. Since the crystals are randomly oriented, collecting patterns on enough crystals (thousands, typically) produces a complete data set of high redundancy for structure determination by molecular replacement (MR) and de novo phasing [4–8]. Data are collected in a sample chamber at atmospheric pressure or in vacuo at 20 °C. Despite the intensity of the X-ray bunch (typically 10^{12}

¹Parts of this chapter are reproduced directly from Ref. [1]

Z. Al-Sahouri · M.-Y. Lee · W. Liu (✉)

Center for Applied Structural Discovery at the Biodesign Institute, School of Molecular Sciences, Arizona State University, Tempe, AZ, USA

e-mail: Zina.Al-Sahouri@asu.edu; minglee@asu.edu; w.liu@asu.edu

D. Li

State Key Laboratory of Molecular Biology, National Center for Protein Science Shanghai, Shanghai Science Research Center, CAS Center for Excellence in Molecular Cell Science, Shanghai Institute of Biochemistry and Cell Biology, Chinese Academy of Sciences, Shanghai, China

e-mail: dianfan.li@sibcb.ac.cn

M. Caffrey (✉)

Membrane Structural and Functional Biology Group, School of Medicine and School of Biochemistry and Immunology, Trinity College Dublin, Dublin, Ireland

e-mail: martin.caffrey@tcd.ie

photons/bunch), each pulse is of such short duration that the changes associated with radiation damage do not progress sufficiently before the diffracted X-rays have departed (*run*) and their structural manifest recorded. We refer to this as “*hit and run*” SFX. It is also known as “*diffraction-before-destruction*” SFX.

The SFX:LCP Marriage A fluid medium is used to ferry crystals of membrane proteins through the pulsed XFEL beam for SFX [4, 8]. Because productive interactions between X-rays and crystals in the flowing stream were so infrequent, typically, only 1 in 25,000 crystals produce a useful diffraction pattern. Thus, vast amounts of valuable membrane protein were required for data collection and most of the protein went to waste. For example, when photosystem I (PSI) crystals dispersed in a continuous liquid jet, data collection required 10 mg of protein [4]. In contrast, when photosynthetic reaction center crystals were dispersed in the more viscous but still quite fluid lipid sponge phase that they had been grown in by the in meso method, only 3 mg of protein were needed [8]. Due to the viscous nature of the mesophases, flow rate would be reduced dramatically. And if suitably high crystal densities in the LCP could be achieved, the rate of delivery of single crystals and X-rays to the interaction region could be matched for a most efficacious use of both. The realization of this idea led to the development of the LCP-SFX method.

Advantages Afforded by LCP-SFX LCP-SFX is appealing as a method because it offers the prospect of obviating some of the issues that arise with in meso-based structure determination using synchrotron X-ray radiation. With the in meso method, crystals are typically grown in a sealed glass sandwich plate. By contrast with crystals grown by the more traditional so-called in surfo methods, their in meso counterparts tend to be considerably smaller. Harvesting crystals from the viscous mesophase is a somewhat cumbersome process that can lead to substantial loss of crystals and to degradation in crystal quality, which may affect diffraction quality. Data collection at a synchrotron source is typically done at 100 K. Such a frigid temperature can stabilize conformational sub-states, particularly in the protein’s side chains, that may not be physiologically relevant and may lead to potential structure–function misinterpretation [9]. Radiation damage is also a major concern when using small crystals with synchrotron radiation sources where residues, such as aspartate and glutamate, are particularly prone to undergo decarboxylation [10]. Damage can be mitigated to a degree with larger crystals, beam attenuation, and data collection at cryo-temperatures, but a complete data set often requires many tens of crystals. In this context then, LCP-SFX is attractive in that it offers an approach to in situ data collection with micrometer or nanometer-sized crystals at or close to the more physiologically relevant 20 °C and the prospect of outrunning the structural consequences of radiation damage.

The LCP as a Liquid Crystal or Mesophase The lipid cubic phase takes center stage in this work. It serves as the medium in which crystallization occurs and is, in turn, used to port those same crystals into the XFEL beam for SFX. As a lyotropic liquid crystal, it is formed most simply by mixing together the monoacylglycerol lipid, monoolein, and water, in approximately equal parts at 20 °C

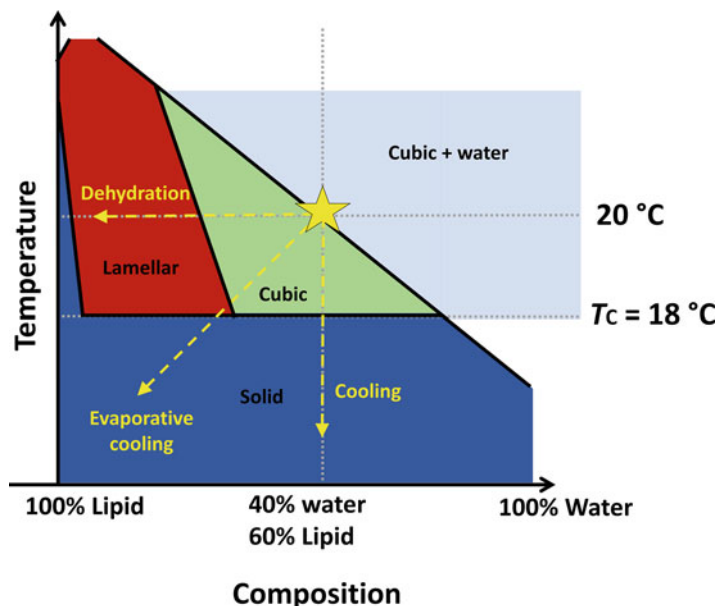


Fig. 4.1 Schematic of the equilibrium temperature–composition phase diagram for the monoolein (9.9 MAG)-water system near 20 °C. The different phases are shown as colored zones and labelled accordingly. The cubic mesophase is extruded into the evacuated sample chamber for SFX under conditions indicated by the yellow star at 20 °C and ~40% aqueous medium. Possible trajectories through the phase diagram taken upon dehydration, cooling and evaporative cooling are indicated by dashed arrows. The 20 °C isotherm is identified by a horizontal dashed line. The liquid crystal-to-solid (Lc) transition is identified by the horizontal dashed line at 18 °C. This schematic is adapted from Ref. [1]

(Fig. 4.1). The hydrophobic effect primarily drives the spontaneous self-assembly of the mesophase. As with any state of matter, mesophase behavior is dictated by Gibbs' phase rule, and is conveniently and concisely summarized in the form of a temperature–composition phase diagram (Fig. 4.1). The equilibrium phase diagram for the monoolein-water system has been mapped out thoroughly based on small- and wide-angle X-ray scattering measurements [11, 12]. Below about 18 °C, cubic phase gives way to a solid, the lamellar crystalline or L_c phase. The cubic phase consists of a single, continuous highly curved and multiply branched lipid bilayer on either side of which is a bathing aqueous channel. These two continuous channels interpenetrate but never contact one another directly because a lipid bilayer separates them. For use in in meso crystallography, the mesophase is prepared typically by combining the host lipid with an aqueous solution of a pure membrane protein solubilized in detergent [13]. The most commonly used host lipids are *cis*-monoenoic monoacylglycerols (MAGs) with acyl chains 14–18 carbon atoms long [14, 15]. Originally, a lipid synthesis program in the Caffrey lab provided these MAGs in support of the in meso method of crystallization [16]. Given their success, many are now commercially available.

Viscosity A noted feature of the cubic phase is its viscosity. The older literature referred to it as the viscous isotropic or VI phase, reflecting its “challenging” rheological and non-birefringent optical properties. Viscosity has been highlighted by some as an undesirable property of the cubic phase as a medium with which to perform crystallization. However, there are several applications where the viscous nature offers distinct advantages. One such example is the use as a medium to transport crystals into the XFEL beam for SFX. Despite its viscosity and challenging handling properties, a robot was built that enables the setting of in meso crystallization trials in high-throughput fashion using miniscule quantities of mesophase and protein [17]. Most trials are set up now using anywhere from 20 to 50 nL of mesophase corresponding to ~5–20 ng protein/well. Given the success of this robot, variations on the original design are available commercially [18].

Rheology Rheology and flow as a jet is dictated to a significant degree by the make-up of the mesophase and in particular the identity of the host MAG component. Different MAGs produce mesophases, each with its own microstructure and physicochemical properties, which will impact uniquely on jet flow and behaviour as a tubular conveyor of crystals. A mesophase with undesirable characteristics might require exorbitantly high and possibly damaging pressures to induce flow. As well, it may produce an unstable jet that breaks up prematurely before reaching the interaction region or curve back out of the beam and onto the nozzle to cause nozzle blockage, interference with flow, and subsequent downtime to correct such issues. A more fluid mesophase will require higher flow rates to produce a stable jet with the added cost of wasted protein crystals as noted above for the sponge phase.

Crystallization Mechanism It is the bicontinuous nature of the LCP that is at the heart of in meso crystallogenesis. Our working hypothesis for how crystallization takes place begins with the target protein reconstituted into and uniformly distributed throughout the continuous, bilayer membrane that permeates the mesophase. Components of the precipitant stabilize a transition locally to the lamellar phase into which proteins diffuse to preferentially partition, concentrate, and subsequently nucleate giving rise to macroscopic crystals [19]. These crystals tend to be generally small, but of high diffraction quality, and considerable effort is usually required to optimize conditions that produce crystals large enough for synchrotron radiation-based data collection.

In Meso Successes to Date Despite the challenges of the method, it has been used to generate crystal structures of a number of different membrane proteins and complexes [13]. The most notable, of late, include the β_2 adrenergic receptor-Gs protein complex that was the subject of the 2012 Nobel Prize in Chemistry [20] and the rhodopsin–arrestin complex [21] (please refer to Chap. 10 for more details). To date, over 400 recorded entries in the Protein Data Bank (PDB, www.pdb.org) are attributed to the in meso method (Fig. 4.2). This corresponds to about 11% of all membrane protein structures deposited in the PDB. Attesting to the growing interest in the method, almost half the in meso PDB records has been added in the past 3 years.

In meso Structures (435)

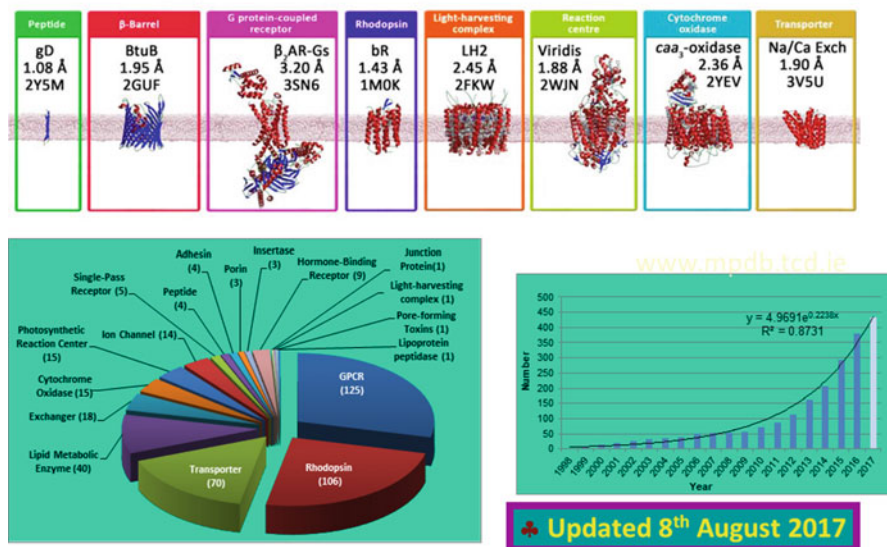


Fig. 4.2 Latest in meso stats

LCP-SFX Technical Challenges Three major technical challenges were identified in implementing LCP-SFX. These included: (1) vacuum incompatibility of the monoolein-based LCP, (2) the need to scale-up from nanoliter to microliter volumes of crystal-laden mesophase, and (3) the provision of an injector that could extrude the highly viscous mesophase in the form of a micrometer-diameter, continuous bolus into the XFEL beam.

Host Lipid, Vacuum Compatibility The first technical challenge relates to the phase behavior of the medium in which crystals are grown and then ported into the XFEL beam for SFX. As noted, data are frequently collected in an evacuated sample chamber at 20 °C. The mesophase containing well-dispersed microcrystals is extruded from the injector as a fully hydrated tubular bolus. Immediately upon entering the chamber, volatiles (water in particular) will evaporate from the surface of the bolus and the sample temperature will drop due to evaporative cooling (Fig. 4.3). Evaporation also leads to the concentration of all non-volatiles in the bolus to increase. These include lipid, detergent, protein, protein crystals, and buffer and precipitant components. Therefore, concentration gradients develop along the length and across the diameter of the cylindrically shaped mesophase bolus. The magnitude of the gradients depends on flow rate and distance along the bolus from the tip of the injector nozzle. Depending on the final concentrations reached, these assorted components can crystallize directly and/or destabilize the dispersing mesophase.

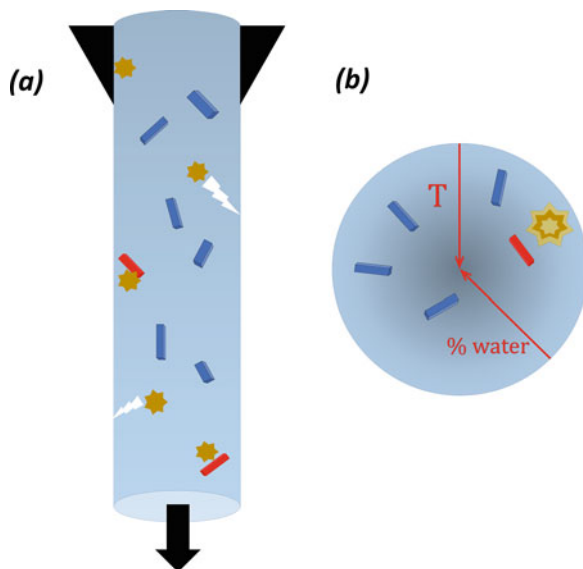


Fig. 4.3 Cartoon representation of the crystal-laden mesophase bolus as it is extruded through the nozzle (black triangles) of the LCP-injector into the evacuated sample chamber at 20 °C for serial femtosecond crystallographic measurements with an X-ray free electron laser. **(a)** Side view of the bolus where the gradient in color from Top to Bottom corresponds to the gradient in temperature and composition along the length of the bolus induced by evaporative cooling. **(b)** End on view of the bolus where the gradient in color corresponds to the gradient in temperature and composition (arrows) along the radius of the cylindrical bolus induced by evaporative cooling. Pristine, undamaged membrane protein crystals are colored blue and are shown dispersed in a light blue cubic mesophase. Stars correspond to sites where the mesophase has transformed from the cubic to the solid Lc phase that may damage the crystals (red) and introduce defects (lightning bolt) in the bolus thereby affecting flow. The enlarged star in **(b)** is drawn to suggest local heating due to the heat of fusion associated with the solidification reaction that may damage dispersed crystals nearby. This schematic is adapted from Ref. [1]

As noted, mesophase behavior is dictated by temperature and composition [11, 12]. Evaporative cooling, brought about by loss of water, will induce sample cooling as well as an increase in lipid concentration. From the equilibrium temperature–composition phase diagram for the monoolein/water system (Fig. 4.1), a reduction in water content together with a drop in temperature will result in a transition from the cubic mesophase to the solid Lc phase [11, 12]. This change in phase can have detrimental consequences such as a change in the rheological and flow characteristics of the extruded jet, creating problems with sample positioning in the XFEL beam. Because the transition has a large associated heat of fusion, wherever crystallization occurs a local “hot” spot will develop that, in turn, may impact negatively on jet flow characteristics and on membrane protein crystal quality. Further, the Lc phase itself, as a solid, may damage the delicate membrane protein crystals dispersed in the bolus. Lastly, Lc phase bolus medium contributes strong

and sharp background powder diffraction at low and wide-angles. Background scatter from the Lc phase creates problems for the recovery of crystal diffraction data from recorded composite images. More importantly, it can damage some detectors, and it is partly for this reason that the incident beam is routinely attenuated some 20-fold during data collection. This is in contrast to the cubic phase, which gives rise to relatively benign diffuse scattering at wide-angles, although diffraction in the low-angle region can be strong and sharp.

It was therefore important to avoid the undesirable cubic-to-Lc transition due to evaporative cooling. An obvious way around this was to reduce the cubic-to-Lc transition temperature, T_c , which could be achieved by using an alternative host MAG to monoolein (9.9 MAG) whose T_c is 18 °C (Fig. 4.1). Separately, we had designed 7.9 MAG (nomenclature described in ref. [22]) for in meso crystallization at low temperatures [23]. The T_c of 7.9 MAG under conditions of full hydration is about 6 °C. This was deemed low enough and 7.9 MAG was chosen as the host lipid for use in a feasibility study with the diacylglycerol kinase, DgkA. It was subsequently shown to behave as expected and to prevent the formation of Lc phase under conditions of SFX data collection.

The 2.05 Å structure of DgkA was obtained using synchrotron X-rays after extensive crystallization screening and optimization [14, 24]. Final crystals were generated in 7.8 MAG at 4 °C. It was necessary therefore to rescreen and optimize in 7.9 MAG, and ideally this should be done at 20 °C, the temperature at which SFX data were to be collected. However, the crystal requirements for synchrotron radiation and for SFX data collection are entirely different. For the former, a few large single crystals suffice. For SFX, tens of microliters of mesophase containing a high density of micrometer-sized crystals are needed.

Adjusting the concentration of 2-methyl-2,4-pentanediol (MPD) in the precipitant solution provided crystals in 7.9 MAG at 20 °C that ranged from showers of microcrystals required for SFX, to isolated, relatively large single crystals suitable for synchrotron radiation data collection. The former were used successfully for SFX and provided a structure of DgkA to 2.18 Å [25]. The latter, however, diffracted at the synchrotron to no better than 6 Å. Additional rounds of optimization, performed at 4 °C, resulted in large, single crystals that provided a synchrotron radiation structure at the same resolution of 2.18 Å [25].

Scaling Up The next technical challenge required increasing the scale of crystallogensis. For SFX, it was anticipated that tens of microliters of crystal-laden mesophase would be required to collect enough data for a structure solution. As noted, in meso crystallization screening is highly efficient and is performed typically on a 50 nL mesophase per well basis [13]. The challenge then was to scale up crystallogensis by about a thousand-fold. Due to a scarcity of membrane proteins generally, extensive screening for optimal crystallization conditions is practically impossible on such a large scale. It is necessary therefore to identify conditions that produce a high density of microcrystals, first under standard conditions in glass sandwich plates at the 50 nL level, and then scale up by a factor of a thousand and hope that the same condition translates directly. However, for the

conditions to translate it is necessary to perform the large volume crystallogensis while maintaining, as much as possible, the same geometrical relationships between mesophase bolus and precipitant solution that prevails during nanoliter volume crystal growth. The geometry in question relates to the shape and size, especially the diameter, of the bolus in contact with the surrounding precipitant solution. Since in meso crystallization has been reasoned to depend on such factors [19], every effort should be made to replicate those conditions for large scale microcrystal production. This can be realized by carrying out crystal growth in a bolus of protein-laden mesophase approximately 15 cm long and 0.4 mm in diameter located toward the center of the barrel of a 100 μ L Hamilton syringe containing precipitant solution. The composition of the precipitant solution would have been identified previously to generate the desired, high density of microcrystals in standard nanoliter-scale glass sandwich plate screening. Upon incubation for a period at 20 $^{\circ}$ C, microcrystals ideally up to 30 μ m long are obtained at a suitably high density. Most of the excess precipitant solution is removed mechanically with the aid of an empty syringe and a narrow bore syringe coupler [26]. The last vestiges of residual excess precipitant are incorporated lyotropically by combining the opaque dispersion with a small volume of host MAG. This procedure generates the required bulk volume of optically clear cubic mesophase in which microcrystals (Fig. 4.4) are uniformly dispersed and ready for SFX measurements in vacuo at 20 $^{\circ}$ C.

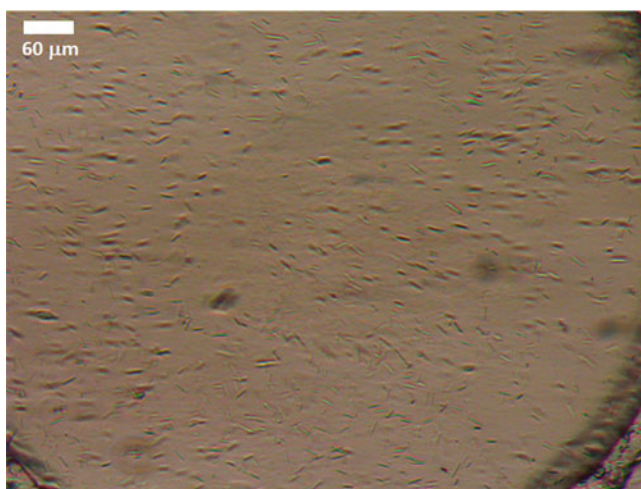


Fig. 4.4 Microcrystals of DgkA grown in the cubic mesophase with 7.9 MAG as host lipid at 20 $^{\circ}$ C in a 0.5 mL syringe. Details of sample preparation are described in Ref. [31]

LCP Injector The third challenge associated with realizing LCP-SFX was the development, building and implementation of an injector capable of delivering the highly viscous, crystal-laden mesophase at a fixed rate as a uniform, continuous, micrometer-diameter, cylindrically shaped bolus to the interaction region in an evacuated sample chamber at 20 °C. Inspired by the simple coupled syringe mixing device used for mesophase preparation and delivery in manual and robotic application of the in meso method, this was realized in the form of the LCP injector [27]. In operation, it involves the extrusion of mesophase from a 20 to 50 μL reservoir through a 6 cm-long glass capillary with an internal diameter of 20–50 μm . The tapered end of the capillary extends beyond the tip of a specially designed gas virtual nozzle which provides a co-flowing stream of gas for reliable, co-axial mesophase extrusion. Pressure, generated by a HPLC pump, is transmitted through water to the mesophase with a pair of Teflon beads separating and providing a watertight seal between the two media. The analogy between the injector and the syringes used in the coupled syringe mixer is striking.

Growing Small Crystals for LCP-SFX The LCP-SFX method introduced in 2013 is robust and well proven. The protocol in place for generating microliter volumes of mesophase with a suitably high density of microcrystals has been described in detail in several publications. An overview of the protocol is outlined below (Fig. 4.5).

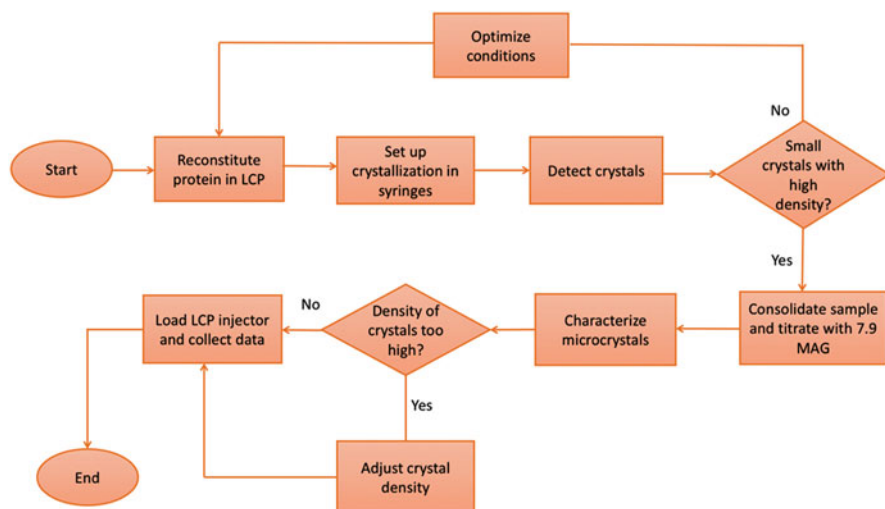


Fig. 4.5 Flowchart summarizing the process of protein reconstitution in lipid cubic phase (LCP) in order to obtain crystals via serial femtosecond crystallography

4.2 Procedure for the Preparation and Characterization of Microcrystals for LCP-SFX

4.2.1 Membrane Protein Reconstitution in LCP (Modified from Ref. [28])

1. Transfer 15 μL of molten 9.9 MAG into syringe no. 1, and 10 μL of protein solution into syringe no. 2.
2. Connect the syringes together using a syringe coupler and homogenize the sample by pushing it through the coupler back-and-forth between syringes, until a transparent LCP forms.
3. To set up crystallization in syringes, move the entire LCP sample into syringe no. 2. Disconnect the empty syringe no. 1, while keeping the coupler connected to syringe no. 2.
4. Attach a removable needle to a 100- μL syringe (no. 3) and aspirate ~ 60 μL of the precipitant solution.
5. Disconnect the needle from syringe no. 3, keeping the Teflon ferrule inside the syringe.
6. Connect syringe no. 3 to the coupler attached to syringe no. 2. Carefully screw and tighten the coupler.
7. Inject ~ 5 μL of protein-laden LCP sample from syringe no. 2 into syringe no. 3 (extruded as a continuous extended string, fully immersed in the precipitant solution).
8. Disconnect syringe no. 3 from the coupler and attach a needle stopper to it. Make sure that LCP does not adhere to the coupler needle during the coupler withdrawal.
9. Use Parafilm strips to seal the needle stopper and the plunger syringe interface to prevent dehydration.
10. Repeat steps 3–8 to set up crystallization in four additional syringes (nos. 4–7).
11. Place syringe nos. 4–7 in a Ziploc bag, and add a moist fiber-free tissue (Kimwipes) to maintain a high level of humidity. Seal the Ziploc bag and store it in a 20 $^{\circ}\text{C}$ incubator.
12. Inspect the samples directly inside syringes every 12 h, using a stereo-zoom microscope equipped with cross-polarizers. Microcrystals typically appear within 1–3 day and can be detected as a faint uniform glow or as densely packed bright dots under cross-polarizers. Microcrystals grown in syringes can be stored for several days at 20 $^{\circ}\text{C}$. Avoid large temperature fluctuations (over 2 $^{\circ}\text{C}$) during sample storage and inspections. Samples in syringes can be transported at this stage to the XFEL source using a Greenbox thermal management system pre-equilibrated at 20 $^{\circ}\text{C}$.

4.2.2 Sample Consolidation and Titration With 7.9 MAG

13. Take out all the samples from the 20 °C incubator ~1 h before the expected start of LCP-SFX data collection.
14. Carefully remove Parafilm seals from syringe no. 3.
15. Replace the needle stopper with a removable needle.
16. Slowly push the plunger of syringe no. 3, squeezing out the precipitant through the needle. Push the plunger of syringe no. 3 slowly and carefully. Abrupt movement can accidentally eject some LCP along with the precipitant solution, resulting in sample loss.
17. Stop pushing the plunger when most of the precipitant solution has been removed.
18. Replace the removable needle with a needle stopper.
19. Repeat steps 13–17 with syringe nos. 4–7.
20. Remove needle stoppers from syringes no. 3 and no. 4 and connect them together using a syringe coupler.
21. Transfer all of the sample from syringe no. 4 into syringe no. 3.
22. Repeat steps 19–20 with syringe nos. 5–7 to consolidate the entire sample in syringe no. 3. Squeeze out as much precipitant as possible.
23. Transfer ~5 μL of 7.9 MAG into a clean 100- μL syringe (no. 2), and connect syringes no. 2 and no. 3 by way of a coupler. The use of 7.9 MAG is only required if LCP is extruded in vacuum for LCP-SFX data collection. When performing LCP-SFX experiments at ambient pressure, 9.9 MAG can be used in this step.
24. Homogenize the sample by moving it through the coupler back-and-forth between syringes.
25. Repeat steps 22–23 until the sample becomes fully homogeneous and transparent. As the exact amount of residual precipitant solution is unknown, 7.9 MAG is titrated in 5- μL increments.
26. Move the entire optically clear sample into syringe no. 2 and disconnect syringe no. 3.

4.2.3 Microcrystal Characterization

27. Attach an LCP injector loading needle (1 in. long, gauge 22, point style 3) to syringe no. 2.
28. Extrude ~1 μL of the sample onto a glass slide, cover it with a glass coverslip and gently press on the coverslip to sandwich the sample.
29. Take images through a high-magnification microscope in bright-field illumination mode and under cross-polarizers. If possible, taking UV fluorescence and SONICC images can help better characterize the sample.

30. Estimate crystal size and density. The minimum crystal size is $\sim 1 \mu\text{m}$. The minimum crystal density that will work depends on the crystal size, the size of the beam, the diameter of the injector's nozzle and the diffraction strength of the crystal. If the crystal density is too high, perform steps 30–34. Otherwise, proceed to step 35.

4.2.4 Adjusting Crystal Density

31. Prepare the volume of LCP as needed for dilution using 50% (vol/vol) 7.9 MAG and 50% (vol/vol) precipitant solution with two clean 100- μL syringes (washed and dried syringes no. 3 and no. 4) and a coupler, as described in step 1.
32. Move the entire 7.9 MAG LCP sample into syringe no. 3. Disconnect syringe no. 4 keeping the coupler connected to syringe no. 3.
33. Connect syringe no. 2, containing the microcrystal-laden LCP, to the coupler attached to syringe no. 3.
34. Homogenize the contents of the two syringes by moving the sample back-and-forth between syringes ~ 100 times.
35. Repeat steps 26–29 to re-evaluate microcrystal size and density.

4.2.5 Loading the Sample in an LCP Injector for LCP-SFX Data Collection

36. Attach an LCP injector loading needle (1 in. long, gauge 22, point style 3) to syringe no. 2 that contains the final LCP sample homogeneously filled with microcrystals.
37. Transfer the sample into an LCP injector.
38. Insert the LCP injector loaded with sample into the sample chamber, start the injector, adjust the LCP flow rate based on the XFEL repetition pulse rate and the detector readout rate, and collect LCP-SFX data.

Issues Issues arise with occasional large crystals present in the mesophase sample. It will/can block/clog the delivery nozzle and can halt the experiment at great cost in failure to use valuable beam time and sample. Also, strong diffraction from big crystals can damage the detector leading to permanently dead pixels. It is partly for this reason that the beam is attenuated to 5–10% of full intensity, which represents underutilization/inefficient use of a very valuable resource, XFEL photons.

Dust and lint will also clog the nozzle and require special sample treatment to avoid. This includes filtering lipid, buffer and precipitant solutions, use of lint-free paper, and working in a relatively dust-free environment.

Not all proteins produce small crystals and optimization may be needed to generate small crystals for use in LCP-SFX. There is also the need to generate a

suitably high density of crystals to increase the single crystal hit rate. Unfortunately, the higher density brings with it a rise in wasted protein between shots.

Crystal Detection and Mensuration It is one thing to grow small crystals. It is another altogether to detect and visualize them. Detection is integral to the success of the downstream SFX measurement and it must be done ideally in a quantitative manner. Thus, not only are crystal dimensions needed with some accuracy, it is also desirable to know the distribution of sizes and crystal density. The methods that have been used to date for these purposes include bright field and cross-polarized light microscopy, UV-fluorescence microscopy, and second order nonlinear imaging of chiral crystals (SONICC). Each comes with its pros and cons. Bright field microscopy is simple and accurate but the size limit extends only to that of light microscopy, which is in the vicinity of 1 μm . Polarizing light microscopy can help with visualization provided the crystal is birefringent. The stronger the birefringence, the smaller the crystal that can be seen. Even still, the method is limited to a resolution of about 1 μm . Unfortunately, optically isotropic crystals with cubic space group symmetry are not birefringent. UV-fluorescence is a very powerful method with a size limit possibly extending to a little below 1 μm . However, it requires that the protein contains amino acids that fluoresce upon excitation with 280 nm light. Tryptophan is the most fluorescent of the amino acids and the more tryptophans in the protein the higher the fluorescence yield and the more sensitive the measurement. For proteins that lack tryptophan, a high tyrosine content may compensate, to a limited degree. An alternative is to trace fluorescently label the protein, which involves separate chemical and purification steps and the introduction of heterogeneity into the sample. SONICC has been used successfully to visualize small membrane protein crystals growing in meso for use in SFX. An advantage of the method is that it has a spatial resolution that extends to <1 μm . Further, it has been adapted for high-throughput measurements with standard in meso crystallization plates. However, the equipment needed to make a SONICC measurement is expensive, several space groups do not give a SONICC signal (providing false negatives) and the method suffers from false positives in that non-proteinaceous crystalline materials such as detergents and lipids can give rise to a SONICC signal. Despite the many disadvantages, the information forthcoming from SONICC is considered sufficiently valuable that an instrument has been installed at the European XFEL. Other methods, such as light scattering and electron microscopy that are used extensively in characterizing crystals of soluble proteins for SFX measurements, thus far have not found application with mesophase grown crystals.

4.3 Results

A feasibility study of the LCP-SFX method was conducted using the coherent X-ray imaging (CXI) instrument at the Linac Coherent Light Source (LCLS) over the course of seven 12-h data collection shifts in March 2013. The CXI

operating conditions included: photon energy, 9.5 keV; wavelength, 1.3 Å; fluence, 10^{12} photons/pulse; average pulse energy at the sample, 0.05 mJ; bunch delivery rate, 120 Hz; pulse length, 50 fs; X-ray focus, 1.5 μm; attenuation, 3–6% of full beam. The injector operated at an effective pressure up to 10,000 psi and a constant volumetric flow rate of 170 nL/min, corresponding to a linear flow rate of 1.4 mm/min. The extruded bolus diameter was ~50 μm as defined by the 50 μm internal diameter of the nozzle capillary. The X-ray beam intersected the mesophase bolus ~100 μm from the tip of the capillary extending from the injector nozzle. The evacuated sample chamber operated at 10^{-4} Torr and 20 °C. Diffraction data were collected on Cornell-SLAC Pixel Array Detector (CSPAD) detectors at sample-to-detector distance of 122 cm. Images and diffraction data were analyzed and processed following published procedures [29–31].

The data required to solve a structure of the test protein DgkA by molecular replacement were collected using approximately 4 h of beam time, 42 μL mesophase, and 200 μg protein. Data collection was greatly facilitated by the high hit rate provided by the LCP jet. The SFX structure, at ~2.18 Å resolution, is very similar to the corresponding structures determined using synchrotron radiation at 100 K. In addition, during the beam time for this feasibility study, structures were obtained for two liganded G protein-coupled receptors (GPCRs) [14].

The use of the LCP-SFX method with GPCRs is described in detail in Chap. 10. One example, 5-HT_{2B}, is a member of the class A GPCR superfamily. The purified 5-HT_{2B}/ergotamine complex was prepared following the protocol described above. Conditions with magnesium sulfate were optimized further to obtain relatively large crystals for traditional microcrystallography at a synchrotron source [32], whereas conditions with magnesium chloride, which reproducibly yielded high-density microcrystals, were used to prepare samples for LCP-SFX [21, 33].

Crystals optimized for traditional crystallography were collected directly from LCP using MiTeGen micromounts and flash-frozen in liquid nitrogen. Crystallographic data were collected at the 23ID-D beamline of the Advanced Photon Source (APS; Argonne, Illinois, USA) using a 10-μm minibeam at a wavelength of 1.0330 Å and a MarMosaic 300 charge-coupled device (CCD) detector. Data from the 17 best crystals collected under cryo-conditions were merged and used to solve the structure by molecular replacement at 2.7 Å resolution [32]. LCP-SFX data were collected at the CXI end station at the LCLS, using 50-fs X-ray pulses (3×10^{10} photons/pulse) at a repetition rate of 120 Hz and a wavelength of 1.3 Å, focused to a 1.5-μm spot size by Kirkpatrick–Baez mirrors. LCP with randomly dispersed 5-HT_{2B}/ergotamine microcrystals was extruded through a 20–50 μm-diameter nozzle into a vacuum chamber at room temperature and at a constant flow rate of 50–200 nL/min, to intersect with the XFEL beam. Single-shot diffraction images were collected using a CSPAD located at a distance of 100 mm from the sample. The structure was determined by molecular replacement to 2.8 Å resolution [32].

Prospects Clearly, the LCP-SFX method for membrane proteins works and will continue to be used with a host of important membrane proteins and complexes,

particularly where sufficiently large crystals cannot be grown for synchrotron radiation diffraction experiments. While the accessibility of LCP-SFX to the scientific community is currently limited by the small number of XFEL sources worldwide, SFX and XFEL have many desirable features, such as beam intensity, reduced radiation damage, and the ability to collect diffraction data from many crystals in a high-throughput manner without the need for mounting single crystals individually. It is expected that these advantages will make use of XFELs more attractive—for soluble as well as membrane proteins. Some thoughts along the lines of how future SFX studies might be improved are presented below.

A detector with wider dynamic range would certainly be of great benefit given that the current CSPAD requires the beam to be attenuated by a factor of ~ 20 to prevent damage from strong and sharp reflections. The latter derive, in part, from the occasional larger membrane protein crystals. Of equal import is detector damage from the solid Lc phase induced to form by evaporative cooling of the host LCP. If an evacuated sample chamber will be used for future LCP-SFX studies then a better understanding is needed of, with a view to controlling, the conditions that prevail in the extruded bolus under data collection conditions. These include knowing the temperature and composition along the length and across the diameter of the bolus and how this impacts phase behavior of the various components therein. The focus must be on mesophase behavior and how this is affected by changes in lipid hydration and temperature, with reference to the relevant temperature–composition phase diagram. The problem of converting to the solid Lc phase can be averted by using a lipid, 7.9 MAG for example, with a lower cubic-to-solid phase transition temperature (T_c). There are other MAGs with low T_c values that can be used for this purpose. An alternative approach, implemented successfully with GPCRs, involves doping mesophase prepared with a different host lipid or lipid mixture in which microcrystals had already grown and were dispersed with the low- T_c 7.9 MAG. Monoolein containing 10 mol% cholesterol was the lipid mixture used in the GPCR application, and 7.9 MAG was added to the extent of 30 mol% post-crystal growth. The preexisting crystals apparently do not suffer any deterioration in diffraction quality as a result of the doping and mixing exercise. However, for this to be a generally applicable procedure checks on crystal quality must be performed and, as needed, doping and mixing protocols where damage is avoided or minimized must be developed. Should the post-crystal growth doping approach work with other host lipids and lipid mixtures, it will expand the space available for crystallization screening enormously in that screening will not be tied to a specific host lipid.

As noted, a synthesis program in the Membrane Structural and Functional Biology Group provides rationally designed lipids for in meso crystallization and other applications in the membrane structural and functional biology field [16, 22, 34]. Separately, MAGs similar to those employed in the field to date and other lipid types have been designed and synthesized for use in low temperature crystallogenesis that may find application in future LCP-SFX studies. To do so, they must be shown to be effective hosting lipids for in meso crystallization and to form a crystal transport medium that is stable to evaporative cooling that takes

place during SFX data collection in vacuo. Alternatively, they might be used to dope microcrystal-mesophase dispersions thereby lowering the effective T_c and preventing evaporative cooling-driven solidification, as already demonstrated with GPCRs [14, 32, 35].

The cubic mesophase, with its rheological hallmark of viscosity, is integral to LCP-SFX. However, not all in meso screening efforts generate structure-quality crystals in the cubic phase. As often as not, the much more fluid, yet bicontinuous sponge phase is the medium from which final crystals emerge [13, 36]. The sponge phase evolves from the cubic phase in the presence of certain precipitant components such as PEG 400, MPD, and butanediol, and appears more prone to form with the shorter chain host MAGs [14]. It is characterized by significantly enlarged aqueous channels, long-range disorder, optical clarity, non-birefringence, and fluidity. It is the latter property that makes it inefficient as an SFX medium [8]. However, the process can be reversed to induce a sponge-to-cubic phase transition. These methods are used, for example, to facilitate crystal harvesting which is generally easier in the viscous cubic phase. The conversion is relatively easy to do when the “spongifying agent” is an additive such as MPD where, typically, reducing the spongifier concentration in the sponge phase by dilution is sufficient to recover the cubic phase. Such an approach might be taken for LCP-SFX when final microcrystals only form in the sponge phase. Presumably, the conversion would be implemented immediately prior to running the SFX measurement and only in situations where it was shown that the process did not compromise crystal quality.

It is important to recognize that the limit to the size of crystals with which quality data can be collected using synchrotron radiation continues to drop as brighter and more intense X-ray beams are produced enabling the creation of smaller beams and as better detectors become available. It is now routine to collect synchrotron data on crystals just 10–50 μm in maximum dimension. Indeed, with new and improved synchrotron beams in the offing, crystals with single digit micrometer dimensions may well provide useful samples for routine data collection.

The in meso method is used primarily for crystallizing membrane proteins. However, it works also with soluble proteins. Lysozyme, thaumatin, and insulin are cases in point [37, 38]. It makes sense therefore to explore the utility of the LCP as a viscous, slow “flowing” medium in which to port microcrystals of soluble proteins and complexes into the XFEL for efficient, high hit-rate SFX. Crystals can be grown in situ and used, essentially, as with membrane proteins. The alternative is to combine extant crystals with preformed mesophase to create a dispersion that can be loaded directly into the reservoir of the LCP injector for SFX measurement. In this latter case, the mesophase would best be prepared with the mother liquor in which the soluble protein crystals grew. As with membrane proteins, MAGs having different acyl chain characteristics and correspondingly different mesophase microstructures and rheologies should prove useful for generating and porting crystals of the widest possible range of soluble protein targets.

Mixing crystals grown by the more traditional in surfo method may be the only possibility for certain membrane proteins. If these only yield microcrystals unsuitable for use with synchrotron radiation and are in short supply where the

more wasteful liquid delivery system is not practical, then using LCP-SFX may be the option of last resort. In this case the extant microcrystals, dispersed in a liquid mother liquor, can be mixed with mesophase, ideally equilibrated with an appropriate mother liquor, and the crystal-laden mesophase used for SFX. The crystals would need to be stable to such a treatment, of course, and conditions may need to be adjusted to find those suited to producing a useful crystal dispersion.

Some proteins are difficult, if not impossible, to optimize to larger size and these would naturally lend themselves to LCP-SFX work. Rhodopsin–arrestin is a particularly compelling example of this. It may also be that with certain proteins or complexes growth is prohibitively slow. Using smaller crystals that can be grown in a reasonable time period would make sense especially if structures were needed for high-throughput screening purposes such as drug design, discovery and development where too slow a growing process could render the project impractical.

Note too that any protein that crystallizes progresses from an initial nucleus followed by a small and then a bigger crystal. It is possible to stop the growth process at a size optimally suited for SFX measurements. However, it may be difficult to stop growth without damaging extant crystals. A simpler solution might be to halt the growth process by using them directly at an intermediate stage in the growth process when crystals are suitably sized for SFX. However, if SFX is to be performed at RT the option of cryopreservation at an intermediate stage of growth is not available and crystals would need to be processed by SFX immediately as they achieve the right size. This would likely mean having to grow crystals on-site and using them for measurement as they matured—a luxury available to a select few.

In the interest of completeness it is appropriate to consider the alternatives to LCP-SFX, the most obvious of which is LCP synchrotron-based serial crystallography (LCP-SSX). LCP-SSX can be done in both fixed and moving target mode. The latter involves using the LCP injector to flow crystal-laden mesophase across a synchrotron X-ray beam. The feasibility of this approach has been demonstrated at several synchrotron facilities and has been shown to work with the model protein bacteriorhodopsin [39]. As with any flowing jet methodology, the process is wasteful requiring large amounts of protein, lipid and ligand if present. The fixed target approach has been implemented in several ways. The *in meso in situ* serial X-ray crystallography (IMISX) method where data are collected at cryogenic temperatures (IMISX_{cryo}) is particularly effective and routinely used in the Caffrey lab. The method dispenses with the need for the technically demanding, inefficient, and potentially damaging crystal (loop) harvesting step that is an integral part of the traditional *in meso* method. For the IMISX method, crystals are grown in a bolus of mesophase sandwiched between thin plastic windows. The bolus contains tens to hundreds of crystals, visible with an *in-line* microscope at the MX synchrotron beamline and suitably disposed for conventional or serial crystallographic data collection. Wells containing the crystal-laden boluses are removed individually from hermetically sealed glass plates in which crystallization occurs, affixed to pins on goniometer bases and excess precipitant removed from around the mesophase. The wells are snap cooled in liquid nitrogen, stored and shipped in Dewars, and manually or robotically mounted on a goniometer in a cryo-stream for diffraction data

collection at 100 K as is done routinely with standard, loop-harvested crystals. The IMISX-cryo approach has been used to generate high-resolution crystal structures of a G protein-coupled receptor, α -helical and β -barrel transporters, and an enzyme as model integral membrane proteins. Insulin and lysozyme were used as test soluble proteins. The quality of data that can be generated by this method has been attested to by performing sulfur and bromine SAD phasing with two of the test proteins. By comparison with the LCP-SFX, the IMISX method can be used with microcrystals, it uses nanogram-to-single digit microgram quantities of protein, there is little if any wasted protein, there are no limitations regarding the type of hosting lipid that can be used for crystallization, it can be used at most synchrotron MX mini-beamlines, it uses materials and instrumentation available for traditional in meso work including robots for setting plates and for mounting samples in the beam, it can be used at both ambient and room temperatures, and in the latter format represents true in situ crystallography in that measurements are made where and as crystals grow.

Crystal structures with ligands bound come at a premium and are much sought after for investigations of mechanism of action and structure-based drug design. Ligands are typically added to the protein before making the mesophase and setting up crystallization trials. They can also be doped into the mesophase to provide an environment for growth that is saturated with ligand. Or crystals of the apo-form can be soaked with ligand directly in meso. In the latter case, smaller crystals may provide an advantage where the surface area to volume (SA/V) ratio is higher for more effective, rapid and complete uptake. Thus, the LCP-SFX approach may prove particularly fruitful for ligand screening in a drug discovery campaign where high-throughput and parallelism is required.

Smaller crystals lend themselves to time-resolved SFX (TRSFEX) where a sudden change in condition, for example, substrate or ligand concentration, can be used to trigger a reaction or a signalling event. The smaller the crystal the larger is the SA/V ratio and the faster is complete saturation of the crystal with ligand, enabling better time resolution.

Smaller crystals also provide advantages with light-activated processes where attenuation in the crystal is less of an issue. This enables a more rapid and uniform initiation of the process throughout the crystal for a more revealing view of the process under investigation. Where this is not possible, the interrogation of multiple states by the beam and their contribution to the measured diffraction signal complicate and may render impossible signal deconvolution and subsequent kinetic analysis.

MR is the phasing method most commonly used in the area of LCP-SFX. However, experimental or de novo phasing that includes S-SAD, is possible with some examples in hand. The requirement in terms of numbers of crystals and amount of protein/ligand for effective de novo phasing is however prohibitive. Only cases where an abundance of protein and ligand is available are likely to benefit from this in the short-term.

Smaller crystals call for smaller jets to reduce background scatter and absorption from the surrounding mesophase thereby maximizing the signal-to-noise (S/N) ratio for better quality data and statistics. However, a jet size that matches that of

the crystal and that maximizes S/N may not be ideal for several reasons. Firstly, the mesophase may be more prone to clogging due to the occasional rogue large crystals and contaminating lint and dust which create costly plumbing problems and instrument downtime. Secondly, because of the larger SA/V ratio, evaporation and evaporative cooling and the attendant problems, as noted above, become more extreme. Thirdly, crystals may suffer from an increased level of mechanical damage as a result of direct contact with the wall of the nozzle capillary and the surface of the jet during delivery. For these reasons using a mesophase jet diameter somewhat larger than the maximum dimension of the dispersed crystals may prove optimal.

4.4 Conclusion

The development of the mesophase and its application as a growing medium for SFX-suitable microcrystals has many advantages. Harvesting crystals is avoided, radiation damage is not a major effect on data quality, and data collection is performed at a biologically relevant temperature. Many advances have been made to use LCP as a medium for SFX, including host lipid selection, development of successful scaling up procedures, and the design of an injector ideal for LCP-SFX, making this a versatile methodology with potential because it fulfills limitations previously involved in crystallizing membrane and soluble proteins.

Acknowledgements This review was supported in part by Science Foundation Ireland (12/IA/1255, 16/IA/4435; M.C.), the National Institutes of Health grants R21 DA042298 (W.L.), R01 GM124152 (W.L.), the National Science Foundation (STC award 1231306) (M.C., W.L.), and the Flinn Foundation Seed Grant (W.L.).

References

1. Caffrey, M., Li, D., Howe, N., & Shah, S. T. A. (2014). 'Hit and run' serial femtosecond crystallography of a membrane kinase in the lipid cubic phase. *Philosophical Transactions of the Royal Society B: Biological Sciences*, *369*, 20130621. <https://doi.org/10.1098/rstb.2013.0621>.
2. Spence, J. C. H., Weierstall, U., & Chapman, H. N. (2012). X-ray lasers for structural and dynamic biology. *Reports on Progress in Physics*, *75*, 102601. <https://doi.org/10.1088/0034-4885/75/10/102601>.
3. Barty, A., Kupper, J., & Chapman, H. N. (2013). Molecular imaging using X-ray free-electron lasers. *Annual Review of Physical Chemistry*, *64*, 415–435. <https://doi.org/10.1146/annurev-physchem-032511-143708>.
4. Chapman, H. N., Fromme, P., Barty, A., White, T. A., Kirian, R. A., Aquila, A., et al. (2011). Femtosecond X-ray protein nanocrystallography. *Nature*, *470*, 73–77.
5. Boutet, S., Lomb, L., Williams, G. J., Barends, T. R., Aquila, A., Doak, R. B., et al. (2012). High-resolution protein structure determination by serial femtosecond crystallography. *Science*, *337*, 362–364.

6. Kern, J., Alonso-Mori, R., Hellmich, J., Tran, R., Hattne, J., Laksmono, H., et al. (2012). Room temperature femtosecond X-ray diffraction of photosystem II microcrystals. *Proceedings of the National Academy of Sciences of the United States of America*, *109*, 9721–9726. <https://doi.org/10.1073/pnas.1204598109>.
7. Redecke, L., Nass, K., DePonte, D. P., White, T. A., Rehders, D., Barty, A., et al. (2013). Natively inhibited Trypanosoma brucei cathepsin B structure determined by using an X-ray laser. *Science*, *339*, 227–230.
8. Johansson, L. C., Arnlund, D., White, T. A., Katona, G., Deponte, D. P., Weierstall, U., et al. (2012). Lipidic phase membrane protein serial femtosecond crystallography. *Nature Methods*, *9*, 263–265. <https://doi.org/10.1038/nmeth.1867>.
9. Fraser, J. S., van den Bedem, H., Samelson, A. J., Lang, P. T., Holton, J. M., Echols, N., et al. (2011). Accessing protein conformational ensembles using room-temperature X-ray crystallography. *Proceedings of the National Academy of Sciences of the United States of America*, *108*, 16247–16252. <https://doi.org/10.1073/pnas.1111325108>.
10. Burmeister, W. P. (2000). Structural changes in a cryo-cooled protein crystal owing to radiation damage. *Acta Crystallographica. Section D, Biological Crystallography*, *56*, 328–341. <https://doi.org/10.1107/S0907444999016261>.
11. Briggs, J., Chung, H., & Caffrey, M. (1996). The temperature-composition phase diagram and mesophase structure characterization of the monoolein/water system. *Journal de Physique II, EDP Sciences*, *6*, 723–751.
12. Qiu, H., & Caffrey, M. (2000). The phase diagram of the monoolein/water system: Metastability and equilibrium aspects. *Biomaterials*, *21*, 223–234. [https://doi.org/10.1016/S0142-9612\(99\)00126-X](https://doi.org/10.1016/S0142-9612(99)00126-X).
13. Caffrey, M., Li, D., & Dukupati, A. (2012). Membrane protein structure determination using crystallography and lipidic mesophases—recent advances and successes. *Biochemistry*, *51*, 6266–6288. <https://doi.org/10.1021/bi300010w>.
14. Liu, W., Wacker, D., Gati, C., Han, G. W., James, D., Wang, D., et al. (2013). Serial femtosecond crystallography of G protein-coupled receptors. *Science*, *342*, 1521–1524. <https://doi.org/10.1126/science.1244142>.
15. Xu, F., Liu, W., Hanson, M. A., Stevens, R. C., & Cherezov, V. (2011). Development of an automated high throughput LCP-FRAP assay to guide membrane protein crystallization in lipid mesophases. *Crystal Growth & Design*, *11*, 1193–1201.
16. Caffrey, M., Lyons, J. A., Smyth, T., & Hart, D. J. (2009). Monoacylglycerols: The workhorse lipids for crystallizing membrane proteins in mesophases. In L. DeLucas (Ed.), *Current topic in membranes* (pp. 83–108). Burlington, NJ: Academic Press.
17. Cherezov, V., Peddi, A., Muthusubramaniam, L., Zheng, Y. F., & Caffrey, M. (2004). A robotic system for crystallizing membrane and soluble proteins in lipidic mesophases. *Acta Crystallographica. Section D, Biological Crystallography*, *60*, 1795–1807. <https://doi.org/10.1107/S0907444904019109>.
18. Li, D., Boland, C., Walsh, K., & Caffrey, M. (2012). Use of a robot for high-throughput crystallization of membrane proteins in lipidic mesophases. *Journal of Visualized Experiments*, *67*, e4000. <https://doi.org/10.3791/4000>.
19. Caffrey, M. (2008). On the mechanism of membrane protein crystallization in lipidic mesophases. *Crystal Growth & Design*, *8*, 4244–4254.
20. Rasmussen, S. G., DeVree, B. T., Zou, Y., Kruse, A. C., Chung, K. Y., Kobilka, T. S., et al. (2011). Crystal structure of the beta2 adrenergic receptor-Gs protein complex. *Nature*, *477*, 549–555.
21. Kang, Y., Zhou, X. E., Gao, X., He, Y., Liu, W., Ishchenko, A., et al. (2015). Crystal structure of rhodopsin bound to arrestin by femtosecond X-ray laser. *Nature*, *523*, 561–567. <https://doi.org/10.1038/nature14656>.
22. Misquitta, L. V., Misquitta, Y., Cherezov, V., Slattery, O., Mohan, J. M., Hart, D., et al. (2004). Membrane protein crystallization in lipidic mesophases with tailored bilayers. *Structure*, *12*, 2113–2124. <https://doi.org/10.1016/j.str.2004.09.020>.

23. Misquitta, Y., Cherezov, V., Havas, F., Patterson, S., Mohan, J. M., Wells, A. J., et al. (2004). Rational design of lipid for membrane protein crystallization. *Journal of Structural Biology*, *148*, 169–175. <https://doi.org/10.1016/j.jsb.2004.06.008>.
24. Wang, C., Jiang, Y., Ma, J., Wu, H., Wacker, D., Katritch, V., et al. (2013). Structural basis for molecular recognition at serotonin receptors. *Science*, *340*, 610–614.
25. Li, D., Stansfeld, P. J., Sansom, M. S. P., Keogh, A., Voageley, L., Howe, N., et al. (2015). Ternary structure reveals mechanism of a membrane diacylglycerol kinase. *Nature Communications*, *6*, 10140 <https://www.nature.com/articles/ncomms10140#supplementary-information>.
26. Cheng, A., Hummel, B., Qiu, H., & Caffrey, M. (1998). A simple mechanical mixer for small viscous lipid-containing samples. *Chemistry and Physics of Lipids*, *95*, 11–21. [https://doi.org/10.1016/S0009-3084\(98\)00060-7](https://doi.org/10.1016/S0009-3084(98)00060-7).
27. Weierstall, U., James, D., Wang, C., White, T. A., Wang, D., Liu, W., et al. (2014). Lipidic cubic phase injector facilitates membrane protein serial femtosecond crystallography. *Nature Communications*, *5*, 3309. <https://doi.org/10.1038/ncomms4309>.
28. Liu, W., Ishchenko, A., & Cherezov, V. (2014). Preparation of microcrystals in lipidic cubic phase for serial femtosecond crystallography. *Nature Protocols*, *9*, 2123–2134. <https://doi.org/10.1038/nprot.2014.141>.
29. White, T. A., Kirian, R. A., Martin, A. V., Aquila, A., Nass, K., Barty, A., et al. (2012). Cryst-FEL: A software suite for snapshot serial crystallography. *Journal of Applied Crystallography*, *45*, 335–341.
30. Kirian, R. A., White, T. A., Holton, J. M., Chapman, H. N., Fromme, P., Barty, A., et al. (2011). Structure-factor analysis of femtosecond microdiffraction patterns from protein nanocrystals. *Acta Crystallographica. Section A, Foundations of Crystallography*, *67*, 131–140. <https://doi.org/10.1107/S0108767310050981>.
31. Kirian, R. A., Wang, X., Weierstall, U., Schmidt, K. E., Spence, J. C., Hunter, M., et al. (2010). Femtosecond protein nanocrystallography-data analysis methods. *Optics Express*, *18*, 5713–5723. <https://doi.org/10.1364/OE.18.005713>.
32. Wacker, D., Wang, C., Katritch, V., Han, G. W., Huang, X.-P., Vardy, E., et al. (2013). Structural features for functional selectivity at serotonin receptors. *Science*, *340*, 615–619. <https://doi.org/10.1126/science.1232808>.
33. Liu, W., Wacker, D., Gati, C., Han, G., James, D., Wang, D., et al. (2013). Serial femtosecond crystallography of G protein-coupled receptors in lipidic cubic phase. *Science*, *342*, 1521–1524. <https://doi.org/10.1126/science.1244142>.
34. Li, D., & Caffrey, M. (2011). Lipid cubic phase as a membrane mimetic for integral membrane protein enzymes. *Proceedings of the National Academy of Sciences of the United States of America*, *108*, 8639–8644. <https://doi.org/10.1073/pnas.1101815108>.
35. Xiang, J., Chun, E., Liu, C., Jing, L., Al-Sahouri, Z., Zhu, L., et al. (2016). Successful strategies to determine high-resolution structures of GPCRs. *Trends in Pharmacological Sciences*, *37*(12), 1055–1069. <https://doi.org/10.1016/j.tips.2016.09.009>.
36. Cherezov, V., Clogston, J., Papiz, M. Z., & Caffrey, M. (2006). Room to move: Crystallizing membrane proteins in swollen lipidic mesophases. *Journal of Molecular Biology*, *357*, 1605–1618. <https://doi.org/10.1016/j.jmb.2006.01.049>.
37. Aherne, M., Lyons, J. A., & Caffrey, M. (2012). A fast, simple and robust protocol for growing crystals in the lipidic cubic phase. *Journal of Applied Crystallography*, *45*, 1330–1333. <https://doi.org/10.1107/S0021889812037880>.
38. Caffrey, M. (2000). A lipid's eye view of membrane protein crystallization in mesophases. *Current Opinion in Structural Biology*, *10*, 486–497. [https://doi.org/10.1016/S0959-440X\(00\)00119-6](https://doi.org/10.1016/S0959-440X(00)00119-6).
39. Nogly, P., James, D., Wang, D., White, T. A., Zatsepin, N., Shilova, A., et al. (2015). Lipidic cubic phase serial millisecond crystallography using synchrotron radiation. *IUCrJ*, *2*, 168–176.